J. Plasma Physics (2010), *vol.* 76, *parts* 3&4, *pp.* 453–466. © Cambridge University Press 2010
doi:10.1017/S0022377809990808

Three-dimensional cylindrical Kadomtsev–Petviashvili equation in a dusty electronegative plasma

W. M. MOSLEM[1], U. M. ABDELSALAM[2], R. SABRY[3], E. F. EL-SHAMY[3] and S. K. EL-LABANY[3]

[1] Department of Physics, Faculty of Science, Port Said, Suez Canal University, Egypt (wmmoslem@hotmail.com)

[2] Department of Mathematics, Faculty of Science, Fayoum University, Egypt

[3] Theoretical Physics Group, Department of Physics, Faculty of Science, Mansoura University, Damietta Branch, New Damietta 34517, Egypt

(Received 28 November 2009, revised 16 December 2009 and accepted 17 December 2009, first published online 29 January 2010)

Abstract. The hydrodynamic equations of positive and negative ions, Boltzmann electron density distribution and Poisson equation with stationary dust particles are used along with the reductive perturbation method to derive a three-dimensional cylindrical Kadomtsev–Petviashvili equation. The generalized expansion method, used to obtain a new class of solutions, admits a train of well-separated bell-shaped periodic pulses. At certain condition, these periodic pulses degenerate to solitary wave solutions. The effects of the physical parameters on the solitary pulses are examined. Finally, the present results should elucidate the properties of ion-acoustic solitary pulses in multi-component plasmas, particularly in Earth's ionosphere.

1. Introduction

For more than three decades, negative ion plasmas attracted attention because of their importance in both laboratory and space observations. In some plasma environments, such as in the Earth's ionosphere [1] and cometary comae [2], the plasma contains both negative ion and positive ion species in addition to electrons. Positive–negative ion plasmas are found in plasma processing reactors [3], neutral beam sources [4] and low-temperature laboratory experiments [5, 6]. Moreover, negative ions were found to outperform positive ions in plasma etching. Therefore, the importance of negative ion plasmas to the field of plasma physics is growing. To treat such plasmas skilfully, basic study and development of diagnostic techniques on negative ion plasmas is indispensable. Recently, Cassini spacecraft has conclusively demonstrated the presence of heavy negative ions in the upper region of Titan atmosphere [7]. These particles may act as organic building blocks for even more complicated molecules. In a negative ion plasma, the number of electrons decreases according to the charge neutrality, i.e. $n_e = n_+ - n_-$, where n_e, n_+, and n_- are the electron, positive ion and negative ion densities, respectively.

The authors dedicate this work to Professor Padma Kant Shukla on the occasion of his 60th birthday.

https://doi.org/10.1017/S0022377809990808 Published online by Cambridge University Press

The resulting decrease in the shielding effect produced by electrons, which is one of the main effects governing the behaviour of plasmas, characterizes the specific phenomena of negative ion plasmas. From this perspective, it seems to follow that the negative ions only influence plasmas secondarily. Although this is a fact, most of the phenomena are actually affected by the negative ions themselves as well as by the lack of electrons [6].

Nowadays, the presence of dust particles has become common and very important factor in solar system, cometary tails, planetary rings, and the evolution of the solar system from its solar nebula to its present form. Experimentally, dust particles are also found in environments such as production processes, flames, rocket exhausts, etching experiments and experiments on dust plasma crystals [8]. Recently, it is found that the presence of negative ions in dusty plasma could change the plasma composition and plasma transport properties [9], as well as the dust charges [10,11]. For example, Kim and Merlino [10] reported the conditions under which dust grains could be positively charged in an electron–ion plasma with both positive and negative ions. Later, positively charged nanoparticles in the night-time polar mesosphere have been observed by Rapp et al. [12]. Rosenberg and Merlino [13] investigated the effect of positive and negative dust grains on the ion-acoustic wave instability in a plasma with negative and positive ions. Thus, the presence of negative ions, as well as either positive or negative dust particles, can produce various nonlinear structures such as solitons and shocks. There remains a wealth of other sources that point towards the existence of dust particles in space observation (cf. [10,13]). Note that the origin and mechanism for the generation of dust particles in space plasma is still an important problem. Therefore, it is of practical interest to examine the effect of dust particles on the properties of the ion-acoustic excitations in positive–negative ion plasmas. Many authors have been investigated similar problems in different systems (e.g. [14,15]). Mamun et al. [16] have investigated the properties of solitary waves and double layers in an electronegative dusty plasma in a planar geometry, and compared the results with experiment [17]. However, to the authors' knowledge, the study of non-planar three-dimensional pulses in multi-component (positive–negative) dusty plasmas has not been examined so far, which is the aim of this work.

This paper is organized as follows. In Sec. 2, we present the governing equations for the non-planar ion-acoustic waves in positive–negative ion plasmas with stationary dust particles. The reductive perturbation method is employed to derive a three-dimensional cylindrical Kadomtsev–Petviashvili (3D-CKP) equation describing the system. In Sec. 3, the generalized expansion method is used to solve analytically the evolution equation and obtain a train of well-separated bell-shaped periodic pulses which can change to solitary pulses at certain conditions. Section 4 contains the numerical results and discussion. Finally, the results are summarized in Sec. 5.

2. Basic equations and derivation of 3D-CKP equation

We consider three-dimensional, collisionless four-component plasmas consisting of positive ions, negative ions, electrons and stationary dust particles. The propagation of the nonlinear electrostatic excitations is governed by a normalized system of fluid equations for the positive and negative ion fluids, distinguished by using the index '+' and '−', respectively. The dynamics are governed by the continuity equations

$$\frac{\partial n_{+,-}}{\partial t} + \nabla \cdot (n_{+,-}\mathbf{u}_{+,-}) = 0, \tag{1}$$

https://doi.org/10.1017/S0022377809990808 Published online by Cambridge University Press

and momentum equations

$$\left(\frac{\partial}{\partial t} + \mathbf{u}_+ \cdot \nabla\right) \mathbf{u}_+ = -\nabla\phi, \tag{2}$$

$$\left(\frac{\partial}{\partial t} + \mathbf{u}_- \cdot \nabla\right) \mathbf{u}_- = Q\nabla\phi, \tag{3}$$

for the two ion species. The Poisson equation reads

$$\nabla^2\phi = n_- - n_+ + n_e - \rho\gamma, \tag{4}$$

and the electron distribution is given by

$$n_e = \alpha \exp\phi. \tag{5}$$

In (1)–(5), $n_{+,-}$ is the positive (negative) ion number density, $\mathbf{u}_{+,-}$ is the positive (negative) ion fluid velocity, ϕ is the electrostatic wave potential. $\rho = +1(-1)$ for positive (negative) dust particles. The variables appearing in (1)–(5) have been scaled by appropriate quantities. Thus, the density n_j (for $j = +, -$, and e) is normalized by the unperturbed positive ion density n_{+0}, $\mathbf{u}_{+,-}$ is scaled by the positive ion sound speed $C_{s+} = (k_B T_e/m_+)^{1/2}$, the potential ϕ is normalized by $k_B T_e/e$. The space and time variables are in units of the positive ion Debye radius $\lambda_{D+} = (k_B T_e/4\pi e^2 n_{+0})^{1/2}$ and the positive ion plasma period $\omega_{p+}^{-1} = (4\pi e^2 n_{+0}/m_+)^{-1/2}$, respectively. We define the mass ratio $Q = m_+/m_-$, where m_+ and m_- are the positive and negative ion masses, respectively. Adopting the neutrality hypothesis, the heavy plasma species density (including positive and negative dust as an ensemble) will be taken to be fixed and continuous, thus providing a globally neutralizing background. The neutrality condition implies

$$1 = \alpha + \beta - \rho\gamma, \tag{6}$$

where $\alpha = n_{e0}/n_{+0}$, $\beta = n_{-0}/n_{+0}$, and $\gamma = Z_d n_{d0}/n_{+0}$. The index '0' denotes the unperturbed density states. Furthermore, Z_d is the magnitude of dust charge.

To investigate the nonlinear propagation of the electrostatic ion-acoustic waves, we shall employ the reductive perturbation method [18, 19]. According to this method, the independent variables can be stretched as:

$$R = \epsilon^{1/2}(r - \lambda t)\,, \qquad \Theta = \epsilon^{-1/2}\theta\,, \qquad Z = \epsilon z, \qquad \text{and} \qquad T = \epsilon^{3/2} t, \tag{7}$$

where ϵ is a small (real) parameter and λ is the wave propagation speed. The dependent variables are expanded as

$$\begin{aligned}
n_{+,-} &= \delta + \epsilon n_{+,-}^{(1)} + \epsilon^2 n_{+,-}^{(2)} + \cdots\,,\\
u_{+,-} &= \epsilon u_{+,-}^{(1)} + \epsilon^2 u_{+,-}^{(2)} + \cdots\,,\\
v_{+,-} &= \epsilon^{3/2} v_{+,-}^{(1)} + \epsilon^{5/2} v_{+,-}^{(2)} + \cdots\,,\\
w_{+,-} &= \epsilon^{3/2} w_{+,-}^{(1)} + \epsilon^{5/2} w_{+,-}^{(2)} + \cdots\,,\\
\phi &= \epsilon\phi^{(1)} + \epsilon^2\phi^{(2)} + \cdots\,,
\end{aligned} \tag{8}$$

where $\delta = 1$ is for positive ions density and $\delta = \beta$ is for negative ions density. In addition, $u_{+,-}$, $v_{+,-}$ and $w_{+,-}$ are the velocities in R, Θ and Z directions,

https://doi.org/10.1017/S0022377809990808 Published online by Cambridge University Press

respectively. Employing the variable stretching (7) and the expansions (8) into (1)–(5), we may now isolate distinct orders in ϵ and derive the corresponding variable contributions. The lowest-order equations in ϵ read

$$n_+^{(1)} = \frac{1}{\lambda^2}\phi^{(1)}, \qquad u_+^{(1)} = \frac{1}{\lambda}\phi^{(1)}, \tag{9}$$

$$\frac{\partial v_+^{(1)}}{\partial R} = \frac{1}{\lambda^2 T}\frac{\partial \phi^{(1)}}{\partial \Theta}, \quad \frac{\partial w_+^{(1)}}{\partial R} = \frac{1}{\lambda}\frac{\partial \phi^{(1)}}{\partial Z}, \tag{10}$$

$$n_-^{(1)} = \frac{-\beta Q}{\lambda^2}\phi^{(1)}, \qquad u_-^{(1)} = \frac{-Q}{\lambda}\phi^{(1)}, \tag{11}$$

$$\frac{\partial v_-^{(1)}}{\partial R} = -\frac{Q}{\lambda^2 T}\frac{\partial \phi^{(1)}}{\partial \Theta}, \quad \frac{\partial w_-^{(1)}}{\partial R} = -\frac{Q}{\lambda}\frac{\partial \phi^{(1)}}{\partial Z}. \tag{12}$$

The Poisson equation provides the compatibility condition

$$\alpha - \frac{1}{\lambda^2} - \frac{\beta Q}{\lambda^2} = 0. \tag{13}$$

The next order in ϵ gives a system of equations in the second-order perturbed quantities. Eliminating the latter and making use of the first-order results, we obtain a nonlinear partial-differential equation in the form of the 3D-CKP equation

$$\frac{\partial}{\partial R}\left(\frac{\partial \phi^{(1)}}{\partial T} + \frac{\phi^{(1)}}{2T} + A\phi^{(1)}\frac{\partial \phi^{(1)}}{\partial R} + B\frac{\partial^3 \phi^{(1)}}{\partial R^3}\right) + \frac{1}{2\lambda T^2}\frac{\partial^2 \phi^{(1)}}{\partial \Theta^2} + \frac{\lambda}{2}\frac{\partial^2 \phi^{(1)}}{\partial Z^2} = 0. \tag{12}$$

The nonlinear and dispersion coefficients are given as

$$A = B\left[\frac{3}{\lambda^4} - \frac{3\beta Q^2}{\lambda^4} - \alpha\right], \tag{13}$$

and

$$B = \left[\frac{\lambda^3}{(2+2\beta Q)}\right]. \tag{14}$$

3. Exact solution to the 3D-CKP equation using generalized expansion method

For simplicity, (12) can be rewritten as

$$\frac{\partial}{\partial R}\left(\frac{\partial \varphi}{\partial T} + \frac{\varphi}{2T} + A\varphi\frac{\partial \varphi}{\partial R} + B\frac{\partial^3 \varphi}{\partial R^3}\right) + \frac{1}{2\lambda T^2}\frac{\partial^2 \varphi}{\partial \Theta^2} + \frac{\lambda}{2}\frac{\partial^2 \varphi}{\partial Z^2} = 0, \tag{15}$$

where $\varphi \equiv \phi^{(1)}$. To find the exact solution to (15), we shall use the generalized expansion method [20]. According to the generalized expansion method, we assume the following ansatz:

$$\varphi = \sum_{i=0}^{2} a_i\, \omega^i \tag{16}$$

and

$$\frac{d\omega}{d\eta} = k\sqrt{\sum_{i=0}^{4} c_i\, \omega^i}, \tag{17}$$

https://doi.org/10.1017/S0022377809990808 Published online by Cambridge University Press

where $k = \pm 1$, a_i are functions in T, c_i are constants to be determined later, and $\omega = \omega(\eta)$. Here $\eta = \alpha_1 R + \alpha_2 \Theta^2 + \alpha_3 Z - U_0 T$, $\alpha_i (i = 1, 2, 3)$ are the functions of T to be determined later and U_0 is a constant speed. We further proceed by substituting (16) into (15) and making use of (17) to obtain a polynomial equation in ω. Equating the coefficients of different powers of ω, we obtain a system of ordinary differential equations, which can be solved with the help of symbolic manipulation package *MATHEMATICA* to give three Jacobi elliptic doubly periodic-type solutions as

$$\varphi = -\frac{\lambda\alpha_3^2 - 2\alpha_1 U_0 + 8B\alpha_1^4 c_2}{2A\alpha_1^2} + \frac{12c_2 Bm^2\alpha_1^2}{A\left(2m^2-1\right)}\ \mathrm{cn}^2\left(\sqrt{\frac{c_2}{\left(2m^2-1\right)}}\eta\right),$$

$$\text{with } c_0 = -\frac{c_2^2 m^2\left(1-m^2\right)}{c_4\left(2m^2-1\right)^2},\quad c_2 > 0,\ c_4 < 0, \tag{18}$$

$$\varphi = -\frac{\lambda\alpha_3^2 - 2\alpha_1 U_0 + 8B\alpha_1^4 c_2}{2A\alpha_1^2} + \frac{12Bm^2\alpha_1^2 c_2}{A\left(m^2+1\right)}\ \mathrm{sn}^2\left(\sqrt{-\frac{c_2}{\left(m^2+1\right)}}\eta\right),$$

$$\text{with } c_0 = \frac{c_2^2 m^2}{c_4\left(m^2+1\right)^2},\ c_2 < 0,\ c_4 > 0, \tag{19}$$

and

$$\varphi = -\frac{\lambda\alpha_3^2 - 2\alpha_1 U_0 + 8B\alpha_1^4 c_2}{2A\alpha_1^2} + \frac{12B\alpha_1^2 c_2}{A\left(2-m^2\right)}\ \mathrm{dn}^2\left(\sqrt{\frac{c_2}{\left(2-m^2\right)}}\eta\right),$$

$$\text{with } c_0 = \frac{c_2^2\left(1-m^2\right)}{c_4\left(2-m^2\right)^2},\quad c_2 > 0,\ c_4 < 0, \tag{20}$$

where $\alpha_2 = -\frac{\lambda}{2}T\alpha_1$ (i.e. $\eta = \alpha_1 R - \frac{\lambda}{2}T\alpha_1\Theta^2 + \alpha_3 Z - U_0 T$) and $c_1 = c_3 = 0$. Note that m is the modulus of the three Jacobi elliptic functions (cn, dn and sn). For $m \to 0$, the Jacobi elliptic functions degenerate to the triangular functions, i.e. sn $\to$ sin, cn $\to$ cos. For $m \to 1$, the Jacobi elliptic functions degenerate to the hyperbolic functions, i.e. sn $\to$ tanh, cn $\to$ sech. Therefore, solutions (18) and (19) degenerate, respectively, to the bell-shaped solitary wave solutions

$$\varphi = -\frac{\lambda\alpha_3^2 - 2\alpha_1 U_0 + 8B\alpha_1^4 c_2}{2A\alpha_1^2} + \frac{12B\alpha_1^2 c_2}{A}\ \mathrm{sech}^2\left(\sqrt{c_2}\,\eta\right),$$

$$\text{with } c_0 = 0,\quad c_2 > 0,\ c_4 < 0, \tag{21}$$

and

$$\varphi = -\frac{\lambda\alpha_3^2 - 2\alpha_1 U_0 + 8B\alpha_1^4 c_2}{2A\alpha_1^2} + \frac{6B\alpha_1^2 c_2}{A}\ \tanh^2\left(\sqrt{-\frac{c_2}{2}}\,\eta\right),$$

$$\text{with } c_0 = \frac{c_2^2}{4c_4},\quad c_2 < 0,\ c_4 > 0. \tag{22}$$

Because c_2 and c_4 are left arbitrary, one may set $\alpha_1 = \ell_\xi$ and $\alpha_3 = \ell_Z$ and take $c_2 = -\left(U_0\ell_\xi - \frac{\lambda}{2}\ell_Z^2\right)/2B$. Hence, the solution (22) reduces to

$$\varphi = \phi_0\ \mathrm{sech}^2\left[\frac{\ell_\xi R + \ell_Z Z - \left(U_0 + \frac{1}{2}\ell_\xi\lambda\Theta^2\right)T}{W}\right], \tag{23}$$

https://doi.org/10.1017/S0022377809990808 Published online by Cambridge University Press

where

$$\phi_0 = 3\left(U_0\ell_\xi - \frac{\lambda}{2}\ell_Z^2\right)/A\ell_\xi^2 \quad \text{and} \quad W = \sqrt{4B/\left(U_0\ell_\xi - \frac{\lambda}{2}\ell_Z^2\right)}. \tag{24}$$

Here, ϕ_0 and W are the maximum amplitude and the width of the solitary pulse. Furthermore, ℓ_ξ and ℓ_Z are the direction cosines ($\ell_\xi^2 + \ell_Z^2 = 1$). Note that $\phi_0 W^2 = 12B/A \equiv$ constant (independent of U_0, though a function of λ). We also see that increasing U_0 leads to an increase in ϕ_0 and a decrease in W, so that taller solitons will be narrower and faster, according to the standard soliton picture [21].

4. Numerical analysis and discussion

Many types of plasmas are present in both space and laboratory experiments. For example, the (H^+, O_2^-) and (H^+, H^-) plasmas have been found in the D and F regions of the Earth's ionosphere. The plasmas with different components will have different mass ratios Q ($= m_+/m_-$), the latter may play a role in the properties of the pulse propagation. Therefore, a part of our analysis investigates the effect of the mass ratio Q on the nonlinear excitations. Numerically, the mass ratios for (H^+, O_2^-) and (H^+, H^-) plasmas are 0.03 and 1, respectively.

Before investigating the behaviour of the nonlinear excitations, we shall first determine the existence condition for localized pulses. For this purpose, we shall express (15) in terms of energy balance equation. Therefore, we use the following transformation $\eta = \ell_\xi R + \ell_Z Z - \left(U_0 + \frac{1}{2}\ell_\xi \lambda\Theta^2\right)T$ to obtain the energy equation as

$$\frac{1}{2}\left(\frac{d\varphi}{d\eta}\right)^2 + V(\varphi) = 0, \tag{25}$$

where the Sagdeev potential $V(\varphi)$ is given by

$$V(\varphi) = \frac{A}{3\ell_\xi^2 B}\varphi^3 - \frac{U_0\ell_\xi - \frac{\lambda}{2}\ell_Z^2}{\ell_\xi^4 B}\varphi^2. \tag{26}$$

For the existence of localized pulse, the condition $d^2V(\varphi)/d\varphi^2 < 0$ at $\varphi = 0$ must be satisfied, which leads to

$$d^2V(\varphi)/d\varphi^2\big|_{\varphi=0} = -2\Delta/\ell_\xi^4 B, \tag{27}$$

where

$$\Delta = U_0\ell_\xi - \frac{\lambda}{2}\ell_Z^2. \tag{28}$$

It is clear from (27) that the localized pulses exist for $\Delta/\ell_\xi^4 B > 0$. However, B is usually positive, so Δ must be greater than zero for the localized pulse existence. To examine the regions for positive Δ, we plot in Fig. 1 the contour of Δ for positive and negative dust particles with α and ℓ_ξ at different values of β. The upper regions of the curves have positive Δ, but the lower regions have negative Δ. For positive dust particles (represented by solid curves), increasing the dust particles concentration α leads to increase in the allowable range of ℓ_ξ, which leads to enhancement of the region for localized pulse existence (i.e. makes the latter much wider). However, increasing the negative ions concentration β makes the region of pulse existence narrower. For negative dust particles (represented by dashed curves), it is seen that when the dust particles concentration α and the negative ions concentration

https://doi.org/10.1017/S0022377809990808 Published online by Cambridge University Press

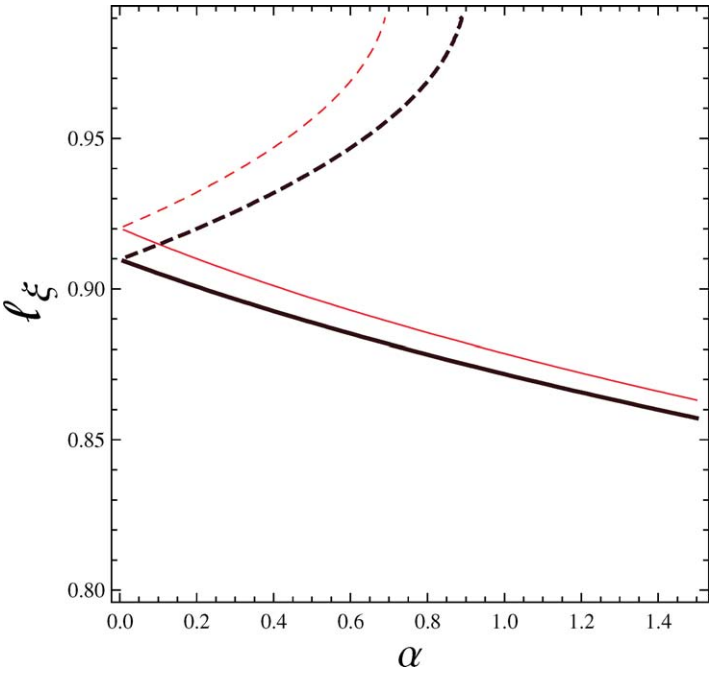


Figure 1. (Color online) The existence regions for the solitary pulses represented by (28) (the contour plot at $\Delta = 0$) for positive dust (solid curves) and for negative dust particles (dashed curves), where $\beta = 0.1$ (thick curves) and $\beta = 0.3$ (thin curves). Recall that the upper region of the curves has only positive Δ (i.e. solitary pulses can propagate) but the lower regions has negative Δ (i.e. solitary pulses cannot exist).

β increase, the pulse can only propagate for a high range of ℓ_ξ and then shrink the allowable region for the localized pulse existence.

Now, we shall investigate the properties of the solitary excitations represented by (12) (which has the solution (23)). Note that the sign of the nonlinear coefficient A affects the sign of ϕ_0, which in turn determines the sign of the potential perturbation $\phi^{(1)} \equiv \varphi$; therefore, both positive and negative pulses may possibly be obtained, for different parameter values, respectively, representing a potential hump or a dip (an electrostatic potential hole). Figure 2 represents the contour plot of the wave amplitude ϕ_0 with γ and β for positive dust particles at $Q = 0.03$ and 1. The light coloured regions correspond to higher (lower) values of the positive (negative) wave amplitude. It is seen that for $Q = 0.03$, the positive potential has a wider region than the negative potential [cf. Fig. 2a]. Increasing the value of Q ($Q = 1$ in Fig. 2b), the negative potential becomes much dominant than the positive potential. Increasing γ leads to decrease (increase) in the positive (negative) wave amplitude. However, increasing β leads to increase (decrease) in the positive (negative) wave amplitude. The contour plot of the wave amplitude ϕ_0 with γ and β for negative dust particles and different values of Q is depicted in Fig. 3. It is obvious that increasing γ and β leads to increase (decrease) in the positive (negative) wave amplitude. From the amplitude expressed by (24), one can see that the numerator of ϕ_0 is identically Δ (which is given by (28)). Recalling that for negative Δ the localized pulse cannot propagate (as a result of the inequality (27)). Importantly, in Figs 2 and 3, it is

https://doi.org/10.1017/S0022377809990808 Published online by Cambridge University Press

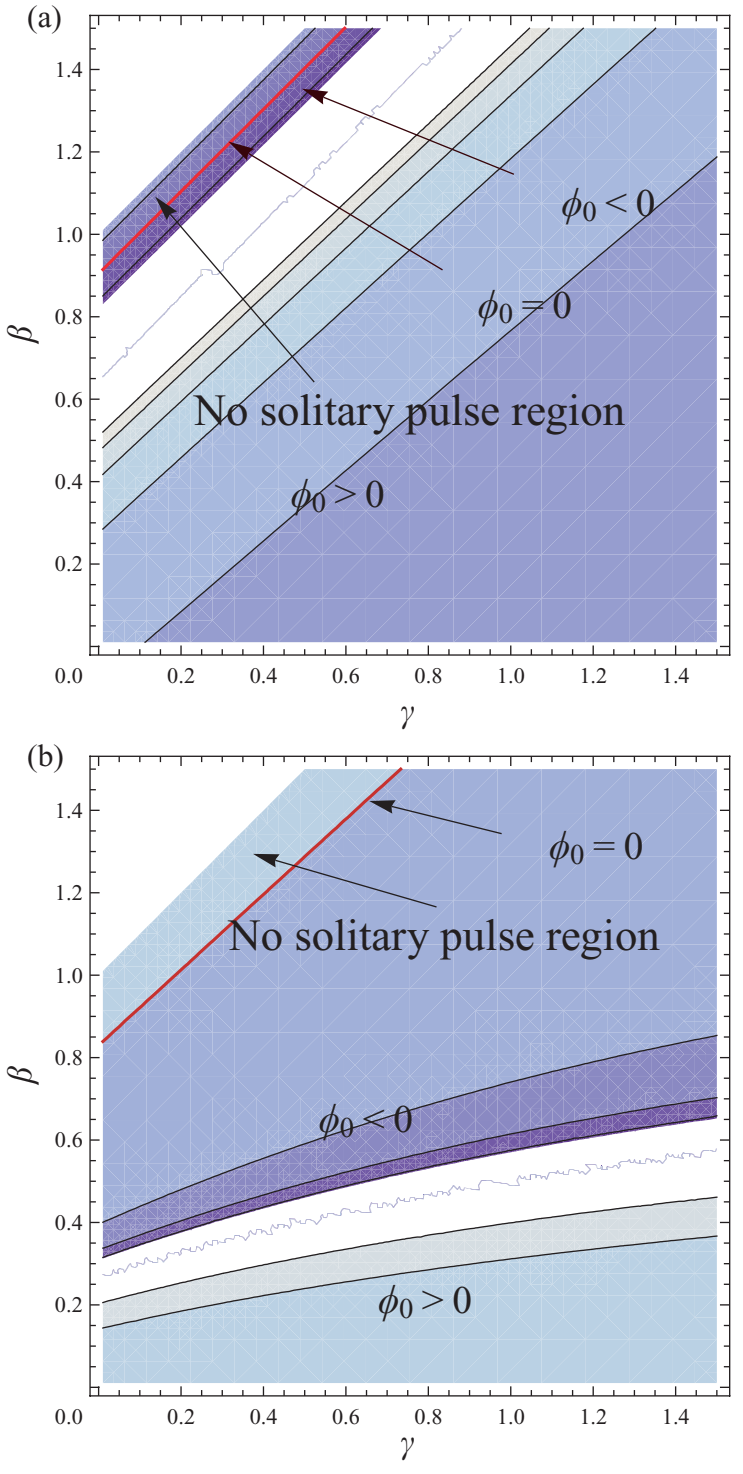


Figure 2. (Color online) The contour plot of the amplitude (given by (24)) with γ and β for positive dust particles, where (a) $Q = 0.03$ and (b) $Q = 1$. Here we have used $\ell_\xi = 0.97$. The light coloured regions correspond to higher (lower) values of the positive (negative) wave amplitude.

https://doi.org/10.1017/S0022377809990808 Published online by Cambridge University Press

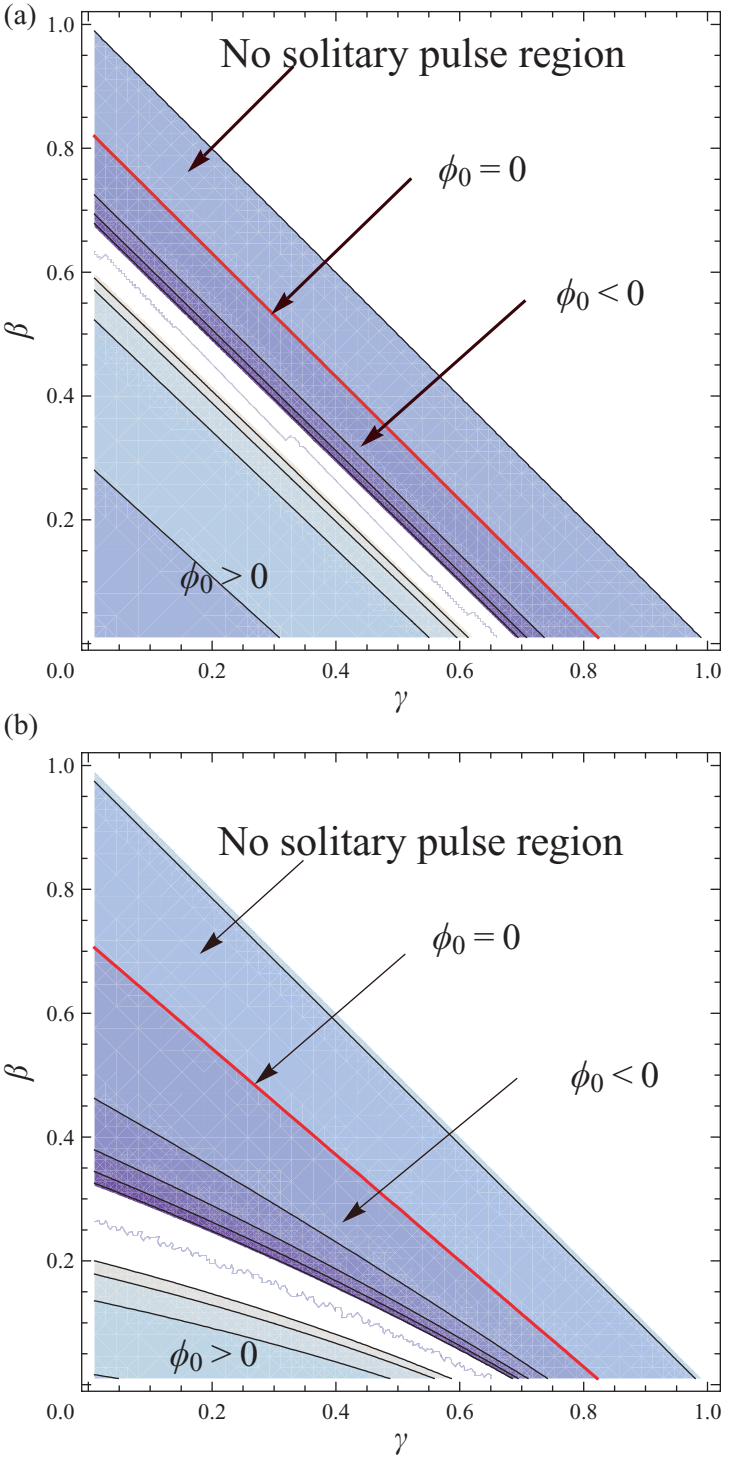


Figure 3. (Color online) The contour plot of the amplitude (given by (24)) with γ and β for negative dust particles, where (a) $Q = 0.03$ and (b) $Q = 1$. Here we have used $\ell_\xi = 0.96$. The light coloured regions correspond to higher (lower) values of the positive (negative) wave amplitude.

https://doi.org/10.1017/S0022377809990808 Published online by Cambridge University Press

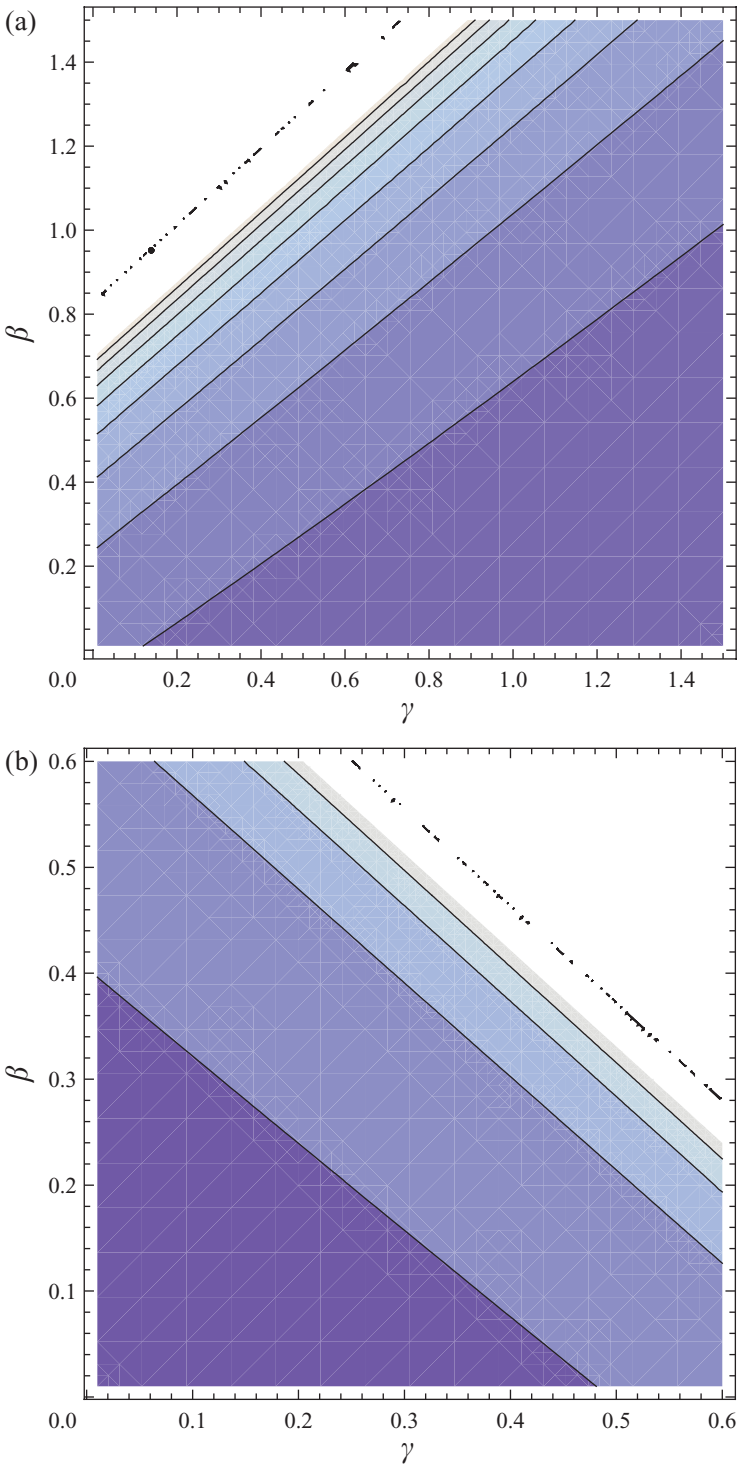


Figure 4. (Color online) The contour plot of the width (given by (24)) with γ and β for (a) positive dust particles and (b) negative dust particles, where $Q = 1$ and $\ell_\xi = 0.96$.

https://doi.org/10.1017/S0022377809990808 Published online by Cambridge University Press

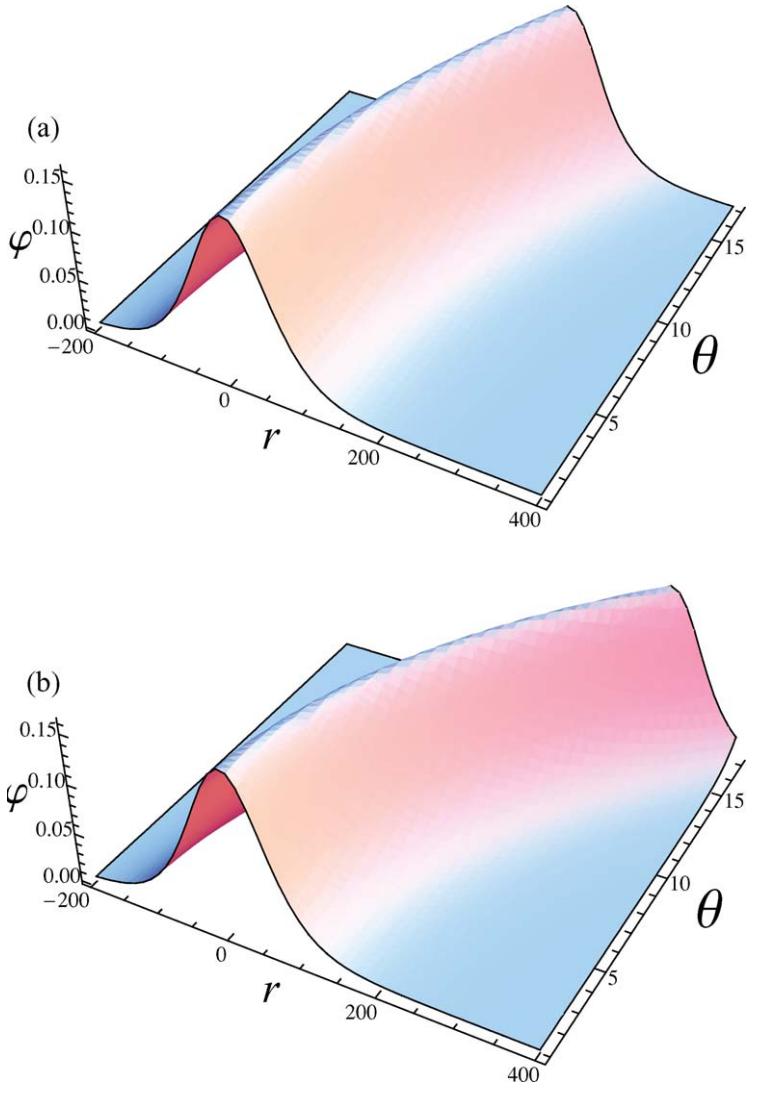


Figure 5. (Color online) The nonlinear ion-acoustic solitary electrostatic potential φ (represented by (23)) is plotted against the radial and polar angle coordinates (r, θ) at different times (a) $t = 1$ and (b) $t = 2$.

seen that at certain values of γ, β and ℓ_ξ, the amplitude becomes zero (because $\Delta = 0$). Behind these critical values (i.e. $\Delta = 0$, the red lines in Figs 2 and 3), Δ becomes negative, which indicates that the pulse cannot propagate for these parameter values. The forbidden regions (i.e. for $\Delta < 0$) of pulse propagating are defined using (28).

The effects of γ and β on the solitary pulse width are depicted in Fig. 4 for $Q = 1$ for simplicity (the case for $Q = 0.03$ has the same qualitative behaviour). It is seen that for positive dust particles (cf. Fig. 4a) the increase of γ (β) leads to shrink (enhance) the pulse width. For negative dust particles (cf. Fig. 4b), increasing both γ and β makes the solitary pulses much wider. Figures 5 and 6 display the

https://doi.org/10.1017/S0022377809990808 Published online by Cambridge University Press

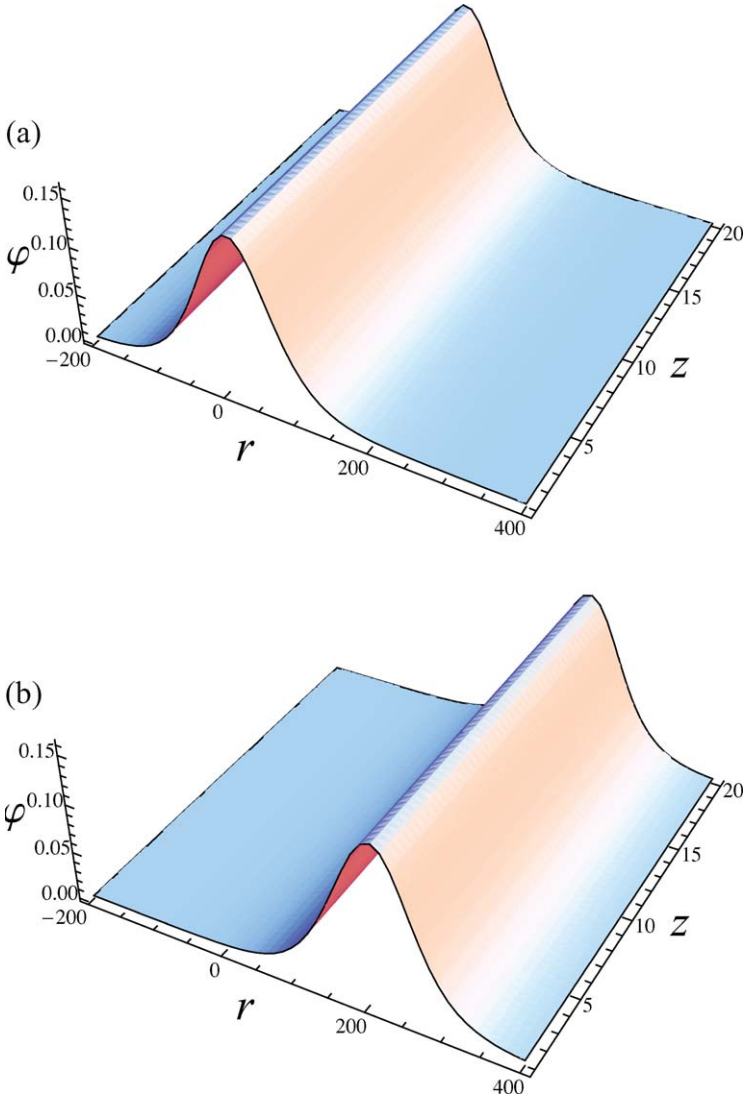


Figure 6. (Color online) The nonlinear ion acoustic solitary electrostatic potential φ [represented by (23)] is plotted against the radial and axial coordinates (r, z) at different time (a) $t = 1$ and (b) $t = 16$.

electrostatic potential with the radial r, angle coordinates θ and axial z at different time t. It is clear that the solitary pulse deviates in the radial direction with the increase of time. Also, as the time goes on, the pulse moves towards the positive radial direction. Of course, such behaviour cannot be noticed in a one-dimensional problem, i.e. neglecting z and θ coordinates and considering the radial part only.

5. Summary

In this paper, the propagation of nonlinear ion-acoustic waves in multi-component dusty plasmas with background stationary dust particles has been investigated.

https://doi.org/10.1017/S0022377809990808 Published online by Cambridge University Press

The evolution of the system was described by the 3D-CKP equation, which solved analytically using the generalized expansion method. According to the generalized expansion method, a new class of solutions to the 3D-CKP equation admits a train of well-separated bell-shaped periodic pulses. At certain condition, these periodic pulses degenerate to solitary pulses. A numerical analysis of the analytical solution revealed that the profile of the nonlinear pulses suffers amplitude and width modifications because of change in the dust particles and negative ions concentrations, as well as positive-to-negative ion mass ratio. Also, the solitary pulse deviates in the radial direction and moves towards the positive radial direction as time goes on. These results would help in understanding the properties of the nonlinear electrostatic structures in the Earth's ionosphere.

Acknowledgements

W. M. M., U. M. A. and R. S. thank the financial support from the ICTP (Italy) during the Summer College on Plasma Physics 2009, where this work was initiated.

References

[1] Massey, H. 1976 *Negative Ions*, 3rd edn. Cambridge: Cambridge University Press, p. 663; Swider, W. 1988 In: *Ionospheric Modeling* (ed. J. N. Korenkov). Basel: Birkhauser, p. 403; Portnyagin, Yu. I. et al. 1992 *Adv. Space Sci. Rev.* **12**, 121.

[2] Chaizy, P. H. et al. 1991 *Nature (London)* **349**, 393.

[3] Gottscho, R. A. and Gaebe, C. E. 1986 *IEEE Trans. Plasma Sci.* **14**, 92.

[4] Bascal, M. and Hamilton, G. W. 1979 *Phys. Rev. Lett.* **42**, 1538.

[5] Jacquinot, J., McVey, B. D. and Scharer, J. E. 1977 *Phys. Rev. Lett.* **39**, 88; Nakamura, Y., Odagiri, T. and Tsukabayashi, I. 2001 *Plasma Phys. Control. Fusion* **39**, 115004; Weingarten, A., Arad, R., Maron, Y. and Fruchtman, A. 2001 *Phys. Rev. Lett.* **87**, 11504.

[6] Ichiki, R., Yoshimura, S., Watanabe, T., Nakamura, Y. and Kawai, Y. 2002 *Phys. Plasmas* **9**, 4481.

[7] Coates, A. J., Crary, F. J., Lewis, G. R., Young, D. T., Waite, Jr., J. H. and Sittler, Jr., E. C. 2007 *Geophys. Res. Lett.* **34**, L22103.

[8] Melandso, F. and Shukla, P. K. 1995 *Planet. Space Sci.* **43**, 635.

[9] Klumov, B. A., Ivlev, A. V. and Morfill, G. 2003 *JETP Lett.* **78**, 300.

[10] Kim, S. H. and Merlino, R. L. 2006 *Phys. Plasmas* **13**, 052118.

[11] Merlino, R. L. and Kim, S. H. 2006 *Appl. Phys. Lett.* **89**, 091501.

[12] Rapp, M., Hedin, J., Strelnikova, J., Friedrich, M., Gumbel, J. and Lübken, F.-J. 2005 *Geophys. Res. Lett.* **32**, L23821.

[13] Rosenberg, M. and Merlino, R. L. 2007 *Planet. Space Sci.* **55**, 1464.

[14] Verheest, F. 2000 *Waves in Dusty Space Plasmas*. Dordrecht: Kluwer Academic; Shukla, P. K. and Mamun, A. A. 2002 *Introduction to Dusty Plasma Physics*. Bristol: Institute of Physics and references therein.

[15] Sayed, F., Haider, M. M., Mamun, A. A., Shukla, P. K., Eliasson, B. and Adhikary, N. 2008 *Phys. Plasmas* **15**, 063701.

[16] Mamun, A. A., Cairns, R. A. and Shukla, P. K. 2009 *Phys. Lett.* A **373**, 2355; Mamun, A. A., Shukla, P. K. and Eliasson, B. 2009 *Phys. Rev.* E **80**, 046406.

[17] Ghim (Kim), Y. and Hershkowitz, N. 2009 *Appl. Phys. Lett.* **94**, 151503.

[18] Washimi, H. and Taniuti, T. 1966 *Phys. Rev. Lett.* **17**, 996.

https://doi.org/10.1017/S0022377809990808 Published online by Cambridge University Press

[19] Xue, J.-K. 2003 *Phys. Plasmas* **10**, 3430.

[20] Sabry, R., Zahran, M. A. and Fan, E. 2004 *Phys. Lett.* A **326**, 93; Sabry, R. and El-Taibany, W. F. 2008 *Nonlinear Analysis* **69**, 2763; Sabry, R., Moslem, W. M., Haas, F., Ali, S. and Shukla, P. K. 2008 *Phys. Plasmas* **15**, 122308.

[21] Dauxois, T. and Peyrard, M. 2005 *Physics of Solitons*. Cambridge: Cambridge University Press, pp. 32–89.

https://doi.org/10.1017/S0022377809990808 Published online by Cambridge University Press